

# Plasticity of rubber-toughened poly(methyl methacrylate): effect of rubber particle size

J. M. Gloaguen, P. Heim\*, P. Gaillard\* and J. M. Lefebvre†

Université des Sciences et Technologies de Lille, Laboratoire de Structure et Propriétés de l'Etat Solide, URA CNRS 234, Bât. C6, 59655 Villeneuve d'Ascq Cedex, France  
(Received 7 January 1992; accepted 17 March 1992)

The plastic deformation of rubber-toughened poly(methyl methacrylate) has been investigated in compression at constant strain rate as a function of particle volume fraction and particle size. The behaviour at yield appears insensitive to particle size for particle diameters  $d$  in the range  $80 \text{ nm} < d < 300 \text{ nm}$ . In contrast, work-hardening rate measurements in the pre-yield region reveal an abrupt change in the material's ability to develop plasticity. This transition from difficult to easy shear-band formation as the rubber volume fraction is varied is shown to occur for the same surface-to-surface interparticle distance, whatever the particle size.

(Keywords: poly(methyl methacrylate); rubber toughening; plasticity; particle size; percolation)

## INTRODUCTION

The mechanical properties of a brittle material such as poly(methyl methacrylate) (PMMA) can be drastically modified by the incorporation of rubber particles. At the expense of a decrease in the yield stress and modulus, one may achieve a noticeable improvement in toughness. The toughening particles are produced by an emulsion polymerization process and then blended into the PMMA matrix. These particles may have different morphologies with alternating layers of rigid PMMA and soft crosslinked rubber, the outer shell always consisting of grafted PMMA<sup>1-3</sup>. The resulting blends may be obtained in all proportions of the rubber volume fraction by melt processing without altering particle structure while ensuring interface continuity due to the inherent miscibility between the PMMA shell and PMMA matrix.

In the present paper, we consider a rubber-toughened poly(methyl methacrylate) (RT-PMMA) with particles of the soft core-hard shell type. Results are reported on the influence of particle volume fraction and particle size on the plastic deformation behaviour at room temperature in compression at low strain rate. Plasticity is viewed in terms of nucleation and propagation of micro-shear zones within the matrix ligaments between the particles. Apart from a classical investigation of the yield stress as a function of these parameters, we develop a characterization of the early stages of the non-elastic deformation through work-hardening rate measurements. It is shown that the latter parameter is a very sensitive tool to probe the microstructural response to plasticity nucleation. After describing the materials under study, we shall recall the theory underlying the work-hardening determination and the corresponding experimental procedure by the so-called direct method. The results will then be discussed in the light of the concepts currently proposed to account

for the toughening mechanisms in rubber-modified polymer systems<sup>4-6</sup>.

## MATERIALS

The PMMA matrix used in all blends has the following molecular mass characteristics:  $M_w = 130\,000 \text{ g mol}^{-1}$  and  $M_n = 65\,000 \text{ g mol}^{-1}$ , as determined by gel permeation chromatography in tetrahydrofuran with a polystyrene calibration. The particles have been prepared by an unseeded semicontinuous process with an elastomer core and a grafted PMMA shell.

The inner crosslinked rubber core is a copolymer of styrene and butyl acrylate with a refractive index which matches that of the PMMA matrix. Details of particle preparation and characterization have been published previously<sup>1</sup>. The PMMA hard layer represents 32.5% of the total particle mass. The three different sizes used in the present work are given in *Table 1* in terms of core and shell diameters,  $d_c$  and  $d_s$ , respectively. Blends have been prepared in a twin-screw extruder with particle weight fractions varying from 5% to 45%. The blend pellets were compression moulded at 200°C into cylinders with a diameter of 8 mm. The slow cooling cycle resulted in samples free from any residual thermal stresses, as checked from the absence of birefringence when viewed between crossed polars. Cylindrical specimens were prepared for compression testing; the dimensions retained are 8 mm in diameter and 16 mm in height, and both ends are finely polished to ensure parallelism to

Table 1 Particle dimensions

Particle	Core diameter (nm)	Shell diameter (nm)
P <sub>1</sub>	87	98
P <sub>2</sub>	183	207
P <sub>3</sub>	241	271

\*Groupement de Recherche de Lacq, BP 34, 64170 Artix, France

†To whom correspondence should be addressed

better than  $10^{-2}$  mm. The large specimen size minimizes experimental scatter at the small non-elastic strains (of a few  $10^{-3}$ ) used.

### PLASTICITY

During compression testing at constant strain rate, non-elastic deformation develops as a heterogeneous process in which micro-shear bands nucleate under increasing stress level, depending on the local degree of steric hindrance, and then propagate to result in a macroscopic assembly of shear bands, as commonly observed at yield. One of the major roles played by the reinforcing particles is to promote extensive shear nucleation, thus reducing the degree of heterogeneity of the deformation and providing a larger energy dissipation capability. The basic idea, when probing the early stages of non-elastic deformation, is to quantify this nucleation step and follow its evolution as a function of particle volume fraction and particle size.

#### The work-hardening rate of solid polymers

Along the lines of this dual nucleation and propagation approach, the evolution of the applied stress  $\sigma_a$  as a function of non-elastic deformation  $\epsilon_p$  is expressed as<sup>7</sup>:

$$\sigma_a = \sigma_i(\epsilon_p) + \sigma_e(T, \dot{\epsilon}_p)$$

in which  $\sigma_i$  accounts for the internal stress field that builds up due to the nucleation of local shear defects with a spatial extent limited to a few neighbouring units. These shear nuclei induce local molecular misfits (stacking faults) whose mutual interactions are at the origin of the rise in  $\sigma_i$  as  $\epsilon_p$  increases in the pre-plastic zone of the stress-strain curve. The local effective stress,  $\sigma_e$ , characterizes the elementary thermally activated shear propagation event. This term is therefore a minor contribution to the applied stress in the pre-yield stage.

Under these assumptions, a structure-dependent parameter is introduced, namely the non-elastic work-hardening rate:

$$K = \left( \frac{\partial \sigma_a}{\partial \epsilon_p} \right)_{\dot{\epsilon}_p, T} = \frac{d\sigma_i}{d\epsilon_p}$$

to probe the ability of a given material to exhibit plastic deformation. Considering that the non-elastic deformation increment  $d\epsilon_p$  results from the nucleation of  $dN$  defects, each contributing an elementary deformation  $e_0$ ,  $K$  can be written as:

$$K = \frac{1}{e_0} \left( \frac{\partial N}{\partial \sigma_a} \right)_{T, \dot{\epsilon}_p}^{-1}$$

i.e.  $K$  is inversely proportional to the number of shear nuclei produced per unit stress. As such, the lower the  $K$  value, the greater is the ability of the material to sustain plastic deformation<sup>7</sup>. The value of  $K$  tends towards zero when one reaches steady plastic flow at yield, whereas it is infinite in the initial elastic portion of the stress-strain curve ( $\epsilon_p = 0$ ).

It has been shown that in between  $K$  varies as  $\epsilon_p^{-1}$ . The  $K$  parameter determined from two stress relaxation tests performed for the same non-elastic strain  $\epsilon_p$  has proved to be a very sensitive tool to follow fine structural evolutions of polymer systems from a deformation point of view. Examples include curing optimization of crosslinked networks<sup>7,8</sup> or evaluation of plasticity

efficiency in glass beads/epoxy composites as a function of interphase structure<sup>9</sup>. In the latter case, an inverse correlation between  $K$  and  $K_{ic}$  values was obtained, thus inferring that the greater shear nucleation rate results in improved toughness. The same correlated variations between work-hardening rate parameter and critical stress intensity factor are evidenced in RT-PMMA. This part of the study is reported elsewhere<sup>10</sup> and refers to  $P_3$  type particles (outer diameter 271 nm).

The relaxation method gives access to a single value of  $K$  for a particular  $\epsilon_p$  and requires two distinct tests to be combined. Considerable improvement has recently been introduced, in both amount of information and accuracy, by work-hardening rate measurements through the so-called direct method<sup>11</sup>. The actual parameter is the slope of the plot of applied stress as a function of non-elastic strain  $\sigma_a(\epsilon_p)$ . Parameter  $K'$  yields the same comparative results of plastic deformation efficiency as  $K$  does, but with a much simpler experimental procedure. The two parameters are related as follows:

$$K' = \left( \frac{\partial \sigma_a}{\partial \epsilon_p} \right)_{\dot{\epsilon}_p} = \frac{d\sigma_i}{d\epsilon_p} + \left( \frac{\partial \sigma_e}{\partial \dot{\epsilon}_p} \right)_T \left( \frac{\partial \dot{\epsilon}_p}{\partial \epsilon_p} \right)_{\dot{\epsilon}_p}$$

in a compression test at constant total strain rate  $\dot{\epsilon}_t$ . If we introduce the stress sensitivity of the strain rate, which has the dimensions of a volume and is measured by a stress relaxation test, i.e.:

$$V = kT \left( \frac{\partial \ln \dot{\epsilon}_p}{\partial \sigma_a} \right)_{T, \sigma_i} = kT \left( \frac{\partial \ln \dot{\epsilon}_p}{\partial \sigma_e} \right)_T$$

one finds<sup>11</sup>:

$$K' = K + \frac{kT}{V} A \quad \text{where} \quad A = \left( \frac{\partial \ln \dot{\epsilon}_p}{\partial \epsilon_p} \right)_{\dot{\epsilon}_p}$$

The procedure is illustrated in the above reference in the case of unsaturated polyester networks and establishes the whole  $K(\epsilon_p)$  curve at a given temperature with a few samples. If one is concerned with classifying materials on the basis of their ability to nucleate plastic deformation, access to  $K'(\epsilon_p)$  alone is sufficient, since both parameters give the same ranking, as has been checked on various polymers (model epoxy networks, unsaturated polyester networks, RT-PMMA) in the laboratory.

### RESULTS

The samples were compression tested at constant strain rate  $\dot{\epsilon}_t = 10^{-4} \text{ s}^{-1}$ . Data acquisition concerned the following parameters: applied stress  $\sigma_a$ , total deformation  $\epsilon_t$  and apparent elastic modulus  $M$ , from which are derived  $\epsilon_p$  and  $K'$ . The data are normalized to unit modulus, in order to compensate for the variation of the latter quantity as the rubber volume fraction is increased. *Figure 1* presents the evolution of  $K'/M$  as a function of  $\epsilon_p$ . The choice of  $\epsilon_p$  to evaluate the influence of volume fraction and/or particle size on  $K'/M$  is arbitrary but obeys the following requirements:

- (i) sensitivity to the prevailing nucleation process necessitates not being too close to the yield point;
- (ii) too small an  $\epsilon_p$  means that a slight variation in  $\epsilon_p$  value results in a large change in  $K'$ , thus increasing error margins on a set of specimens.

For these reasons, a value of  $\epsilon_p = 1.5 \times 10^{-3}$  has been retained to plot the data as a function of the

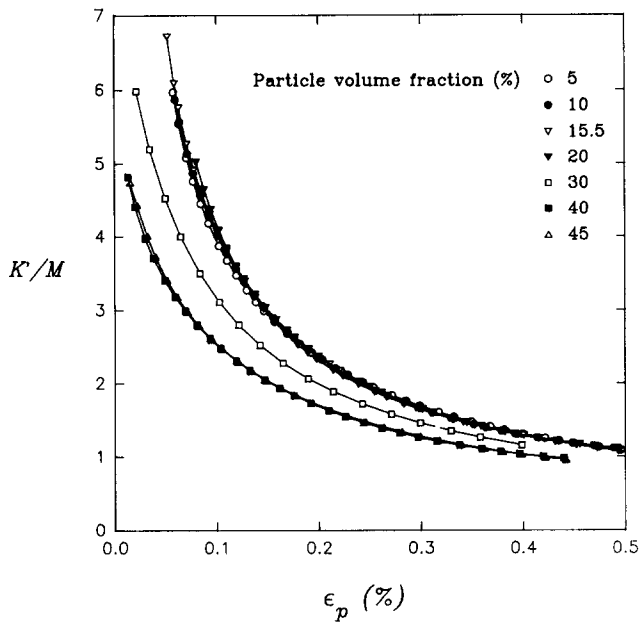


Figure 1 Evolution of  $K'/M$  as a function of  $\epsilon_p$  for blends with particles  $P_3$

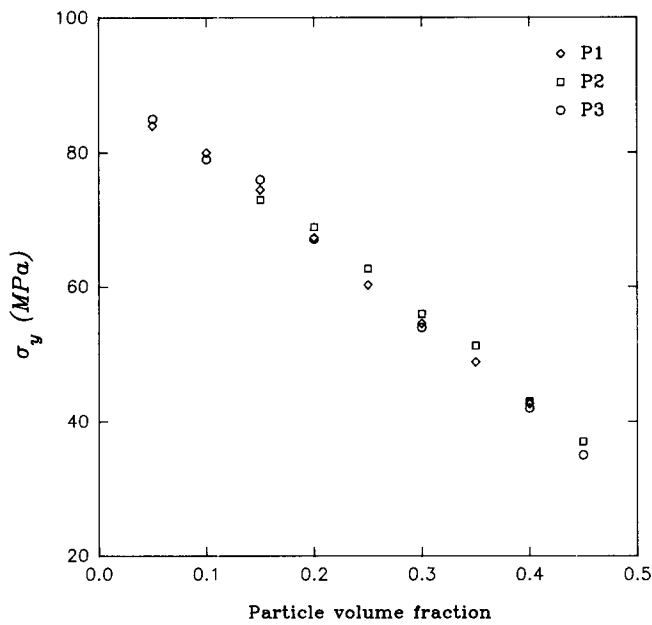


Figure 2 Variation of the yield stress with particle volume fraction

morphological parameters. It corresponds to  $\sigma_a/\sigma_y = 0.6$  in all cases. The tests have been conducted beyond yield so that both nucleation and steady-state shear-band propagation are characterized. The yield stress data are presented in Figure 2 as a function of particle volume fraction for the three different particle sizes. No distinction may be seen to arise from a particle size effect, a feature already mentioned in the case of nylon-rubber blends<sup>5</sup>. In the latter study, although the yield stress was insensitive to particle size, this parameter had a strong effect on the impact behaviour. A model has recently been proposed by Ouali *et al.*<sup>12</sup> to account for the evolution of both the modulus and flow stress of RT-PMMA as a function of rubber content. It is based on a classical series-parallel matrix-rubber association in which introduction of the percolation concept suppresses the need for any adjustable parameter. Calculations

according to the same procedure give the full curve drawn on Figure 3, thus showing fairly good agreement with the reduced yield stress data  $\sigma_{y(\text{blend})}/\sigma_{y(\text{PMMA})}$ .

Prior to considering the work-hardening rate data, we may summarize the results on plastic flow stress as follows:

- (i)  $\sigma_y$  shows a linear decrease with increasing particle volume fraction; and
- (ii)  $\sigma_y$  is insensitive to particle size.

When compared to these results, the data obtained in the pre-plastic stage are quite striking. The values of  $K'/M$  as a function of particle volume fraction are reproduced in Figure 4 for all three particle sizes.  $K'/M$  is taken in all cases at  $\epsilon_p = 1.5 \times 10^{-3}$  as already indicated previously, but the observed evolution is typical of this pre-plastic behaviour. Within experimental errors,

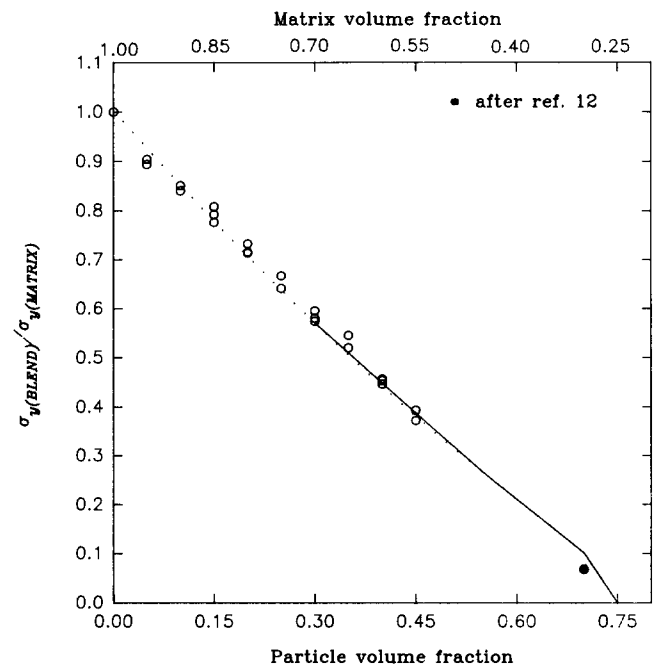


Figure 3 Reduced yield stress data as a function of particle volume fraction (after ref. 12)

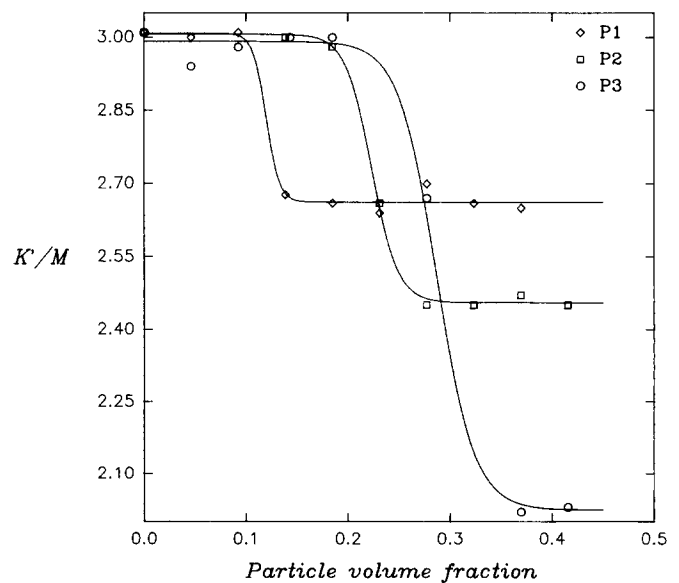


Figure 4 Variation of  $K'/M$  as a function of particle volume fraction for  $\epsilon_p = 1.5 \times 10^{-3}$

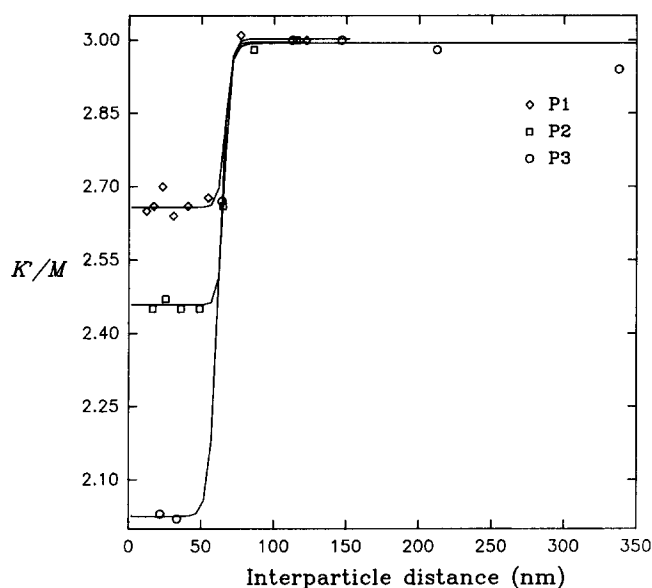


Figure 5 Evolution of  $K'/M$  as a function of interparticle distance

it may be seen that  $K'/M$  starts from an initial upper plateau value common to the whole set of data, followed by a sudden drop, which occurs at a different critical volume fraction, depending on the particle size. A lower plateau value is then reached, the magnitude of the drop being once again dependent on particle size. Before addressing the various aspects of this peculiar shear-band nucleation behaviour, it is worth mentioning that the transition is seen in the same way with either the stress relaxation method<sup>10</sup> ( $K$  parameter) or the present direct method ( $K'$  parameter).

Returning to the significance of the plots illustrated in Figure 4, the work-hardening rate exhibits an abrupt transition from a given state of plasticity nucleation, common to all three systems (and to the pure PMMA matrix), to a state of easier nucleation (drop in  $K'$ ) beyond a certain critical volume fraction.

## DISCUSSION

In a preceding part of this study<sup>10</sup>, we have established the existence of an inverse correlation between work-hardening rate and critical stress intensity factor for crack initiation. The drop in  $K/M$  values was accompanied by an increase in  $K_{Ic}$ . We have thus shown a direct link between pre-plasticity and toughness, whereas no such correlation exists when considering the steady-state flow as seen above or in ref. 5.

In order to recognize the critical morphological parameter operative in these sharp transitions in  $K'/M$  values, the data of Figure 4 have been reconsidered by introducing the matrix ligament thickness approach<sup>4</sup>. The data of Figure 5 yield a single-parameter transition in the  $K'/M$  behaviour, i.e. the drop in work-hardening rate occurs for all three blends at an average critical surface-to-surface interparticle distance  $\tau_c \sim 60$  nm;  $\tau_c$  is taken from shell-to-shell surfaces. As in the brittle tough behaviour of nylon-rubber blends, our plasticity data normalize quite well to Wu's parameter in a simple cubic lattice. What is the significance of  $\tau_c$ ? Obviously in real blends there is a wide distribution of interparticle distances even if, as is the case for RT-PMMA, the distribution of particle diameters is rather narrow.

Moreover the average value obtained for  $\tau_c$  is surprisingly small, i.e. of the order of the radius of the smallest particle ( $P_1$ ), which means that stress field overlap is operative in all blends but at very different magnitudes. Therefore, as already recognized by Wu, a critical stress field overlap cannot explain the transition in plasticity nucleation. Going back to the problem of the distribution of interparticle distances, our results suggest that enhanced local nucleation efficiency is not sufficient. We may then postulate that there is a requirement for connectivity of the ligaments with active shear nuclei to achieve the observed macroscopic property. This percolation problem has been formulated by Sjoerdsma to explain the tough-brittle transition in rubber-modified polymers<sup>6</sup>. He considers the yielded zone ahead of a notch as a rectangular box divided into horizontal layers, the thickness of which is equal to the particle diameter. The blend becomes brittle if the probability of finding an uninterrupted link of unyielded material between the top and bottom of the plastic zone exceeds a critical value. The theory predicts that at the brittle-tough transition  $f^2/d$  should be a constant ( $f$  and  $d$  are the volume fraction and particle diameter respectively), in fairly good agreement with Wu's data<sup>13</sup>. Paralleling this approach with the data of Figure 4 does not, however, provide the same kind of agreement.

Another way to solve the percolation problem is to follow the procedure described by Margolina and Wu<sup>14</sup>, namely the percolation of spherical stress volumes in a random lattice. The stress volume diameter is  $S = d + \tau_c$ . With the present data, the critical particle size  $d_c$  is not known, but the critical volume fraction is. This enables one to calculate the critical stress volume fraction  $\Phi_{sc}$ , which is plotted as a function of  $d/S$  in Figure 6. The value is roughly constant (between 0.35 and 0.40), in agreement with theoretical predictions for monodisperse particles<sup>14,15</sup>. A further test of the validity of applying a percolation model is to check for the existence of a scaling law. This is done in the log-log plot of Figure 7 in which data are analysed as:

$$A_{PMMA}/A_{blend} \sim (\Phi_s - \Phi_{sc})^\beta$$

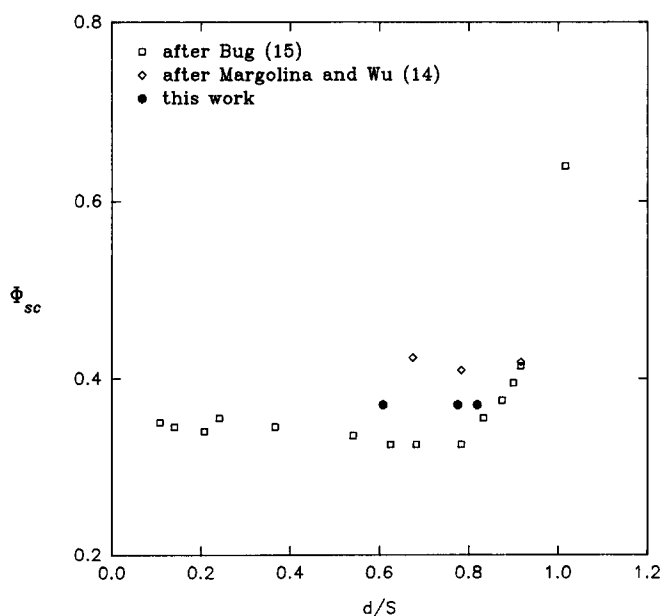


Figure 6 Plot of the critical stress volume fraction as a function of  $d/S$

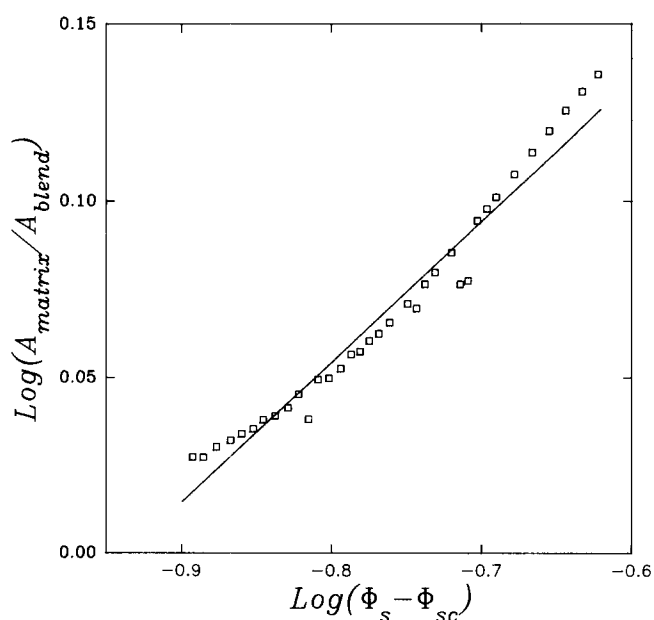


Figure 7  $\text{Log } A_{\text{PMMA}}/A_{\text{blend}}$  versus  $\text{log } (\Phi_s - \Phi_{sc})$

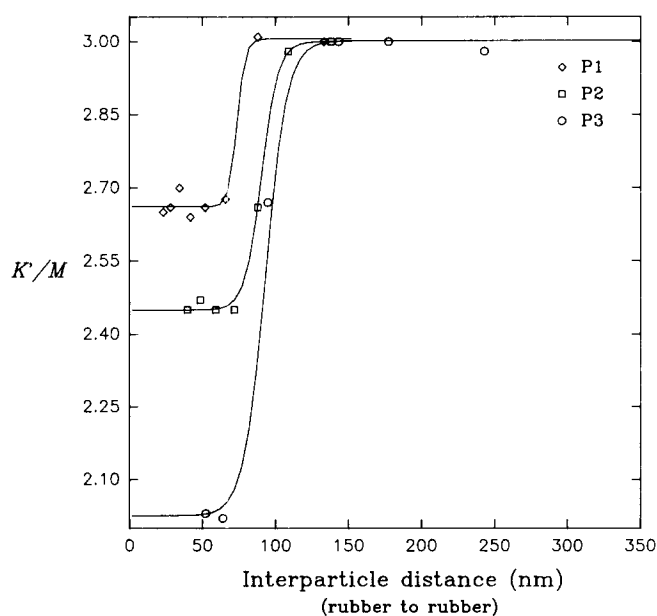


Figure 8 Evolution of  $K'/M$  as a function of interparticle distance (rubber-to-rubber surface)

where  $A$  stands for  $K'/M$ . An increase in this ratio indicates a plasticity improvement. It is worth mentioning that, for each type of particle, this ratio is independent of  $\varepsilon_p$  in the pre-plastic domain where the work-hardening parameter varies roughly as  $1/\varepsilon_p$ .

We find a critical exponent  $\beta = 0.41 \pm 0.05$ , in fairly good agreement with the classical exponent  $\beta = 0.44$  in three dimensions. We have thus provided reasonable evidence for the need for volume connectivity of the plastically active matrix ligaments.

Two more comments have to be made from a materials point of view: First of all,  $\tau_c$  is taken as the outer shell surface-to-surface interparticle distance. It might seem surprising since this hard shell is made of grafted PMMA and is thus miscible with the PMMA matrix. The same plot as in Figure 5, but with  $\tau$  taken as the rubber-to-rubber interparticle distance, presented in

Figure 8, shows differences in the critical parameter beyond experimental error. An explanation may be offered in view of the recent dynamic mechanical study by Ouali *et al.*<sup>12</sup> on the same blends. These authors postulate the existence of an interphase comprising a styrene-butyl acrylate-methyl methacrylate terpolymer with presumably a concentration gradient from the rubber surface to the outer shell surface. In this case additional molecular mobilities in the shell would be operative to trigger shear nucleation within the PMMA matrix.

A second morphological proof of 'selective plasticity' is provided by the work of Bouton-Rochelle and G'Sell<sup>16</sup>. Transmission electron microscopy (TEM) pictures of RT-PMMA samples deformed in either tension or simple shear and quenched under stress reveal the existence of strangely distorted pairs of nodules with a curved tail in regions of very small interparticle distances. Computer simulations of these observations indicate the occurrence of concentrated shear yielding between the particles, with a local deformation as high as eight times the macroscopic one.

Returning to the influence of particle size, we have already established that it affects neither the yield stress  $\sigma_y$  nor the critical interparticle distance  $\tau_c$  for the transition in shear nucleation capability. One aspect is, however, differentiated, i.e. the magnitude of the drop in  $K'/M$  as seen in Figure 5.

If one considers volume fractions for which all blends are in the easy shear nucleation regime (i.e.  $V_f \geq 40\%$ ), it may be seen that  $K'/M$  decreases with increasing particle size, thus indicative of a greater efficiency for the larger particles studied here. This evolution may be compared to that of the critical stress intensity factor  $K_{Ic}$  or critical energy release rate  $G_{Ic}$  observed for similar blends (except for the smallest particle size, which is slightly larger) with a 45% particle volume fraction<sup>2</sup>. Figure 9 evidences again correlated evolutions of toughness and pre-plasticity parameters, as already observed previously<sup>9,10</sup>. The drop in  $K'/M$ , which implies easier shear-banding nucleation, is directly related to improved toughness.

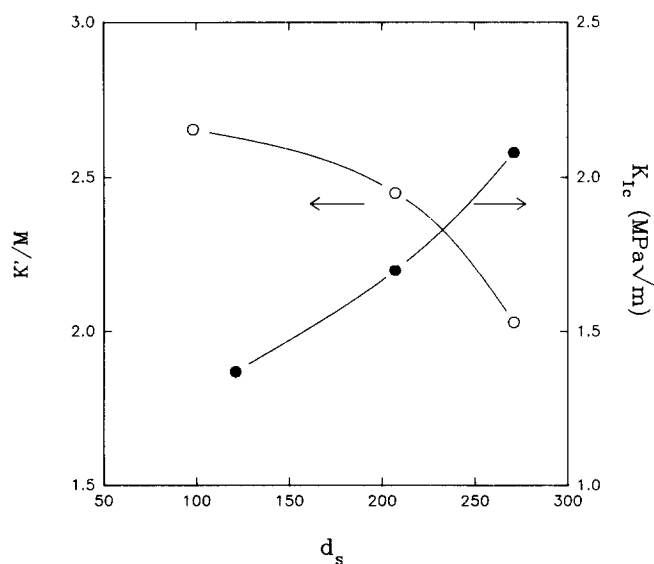


Figure 9 Variation of  $K'/M$  and  $K_{Ic}$  as a function of particle size for  $V_f = 45\%$  ( $K_{Ic}$  data after ref. 2)

## CONCLUSIONS

The present study of the plastic deformation behaviour of RT-PMMA enables us to clarify the respective roles of volume fraction and particle size.

It is shown that yielding (propagation-dominated) is insensitive to particle size in the range  $80 \text{ nm} < d < 300 \text{ nm}$ . However, probing the pre-plastic zone of the stress-strain curve (nucleation-dominated) clearly discriminates the way in which non-elastic deformation responds to variations in the morphological parameters mentioned above. A unique critical interparticle (shell-to-shell) matrix ligament thickness  $\tau_c$  is obtained for all blends and the current data are compatible with a percolation formulation of the connectivity of locally active matrix ligaments to account for the macroscopic non-elastic behaviour.

## ACKNOWLEDGEMENTS

We are grateful to Ministère de la Recherche et de la Technologie for financial support under Programme GIS Alliages de Polymères and for providing a grant to J.M.G. during the course of his PhD work.

## REFERENCES

- 1 Hooley, C. J., Moore, D. R., Whale, M. and Williams, M. J. *Plast. Rubb. Process. Appl.* 1981, **1**, 345
- 2 Wrotecki, C., Heim, P. and Gaillard, P. *Polym. Eng. Sci.* 1991, **31**, 213
- 3 Lovell, P. A., McDonald, J., Saunders, D. E. J., Sherratt, M. N. and Young, R. J. *Plast. Rubb. Process. Appl.* 1991, **16**, 37
- 4 Wu, S. *J. Appl. Polym. Sci.* 1988, **35**, 549
- 5 Borggreve, R. J. M., Gaymans, R. J. and Luttmmer, A. R. *Makromol. Chem., Macromol. Symp.* 1988, **16**, 195
- 6 Sjoerdsma, S. D. *Polym. Commun.* 1989, **30**, 106
- 7 Lefebvre, J. M., Bultel, C. and Escaig, B. *J. Mater. Sci.* 1984, **19**, 2415
- 8 Caux, X., Coulon, G. and Escaig, B. *J. Polym. Sci., Polym. Phys. Edn.* 1987, **25**, 2189
- 9 Amdouni, N., Sautereau, H., Gérard, J. F., Fernagut, F., Coulon, G. and Lefebvre, J. M. *J. Mater. Sci.* 1990, **25**, 1435
- 10 Gloaguen, J. M., Steer, P., Gaillard, P., Wrotecki, C. and Lefebvre, J. M. *Polym. Eng. Sci.* in press
- 11 François, P., Melot, D., Lefebvre, J. M. and Escaig, B. *J. Mater. Sci.* 1992, **27**, 2173
- 12 Ouali, N., Cavallé, J. Y. and Perez, J. *Plast. Rubb. Process. Appl.* 1991, **16**, 55
- 13 Wu, S. *Polymer* 1985, **26**, 1855
- 14 Margolina, A. and Wu, S. *Polymer* 1988, **29**, 2171
- 15 Bug, A. L. R., Safran, S. A., Grest, G. S. and Webman, I. *Phys. Rev. Lett.* 1985, **55**, 1896
- 16 Bouton-Rochelle, C., Thèse de Doctorat, INPL, Nancy, 1991